Biphoton generation enhanced by nonlocal nonlinearity via Rydberg interactions

HUI-MIN ZHAO[1], XIAO-JUN ZHANG[1], M. ARTONI[2,3], G. C. LA ROCCA[4], AND JIN-HUI WU[1,*]

[1] School of Physics and Center for Quantum Sciences, Northeast Normal University, Changchun 130024, China
[2] Department of Engineering and Information Technology, Brescia University, 25133 Brescia, Italy
[3] European Laboratory for Nonlinear Spectroscopy (LENS), 50019 Sesto Fiorentino, Italy
[4] NEST, Scuola Normale Superiore, 56126 Pisa, Italy
[*] jhwu@nenu.edu.cn

Compiled September 6, 2023

Strongly correlated Stokes and anti-Stokes photon pairs (*biphotons*) exhibiting very large generation rates and spectral brightnesses could be attained at extremely low pump powers and optical depths. This is realized via spontaneous four-wave mixing in cold atoms with enhanced nonlocal (Rydberg) optical nonlinearities and prepared into a dark state with a large population imbalance. The scheme works with all light fields on resonance yet with negligible linear absorption and Raman gain.

http://dx.doi.org/10.1364/ao.XX.XXXXXX

Rydberg atoms in highly excited states typically exhibit long radiative lifetimes, large electric-dipole moments, and strong dipole-dipole interactions (DDIs) [1]. These features, significant for both fundamental interest and potential applications, have been well explored to realize quantum gates, quantum memories, single-photon devices, quantum simulation, quantum metrology, etc [2]. Usually manifested as van der Waals (*vdW*) potentials, DDIs offer a promising avenue for the nonlocal control of nonlinear optical responses because they can be easily modulated by changing atomic densities and/or manipulating external fields. Mean-field models are often employed to reduce the calculation complexity of Rydberg atoms [3, 4], though a many-body approach is needed to account for the inter-particle correlations induced by *vdW* interactions [5–7].

Photon pairs or biphotons generated from spontaneous four-wave mixing (SFWM) processes [8–16] are highly required in constructing quantum interfaces between photonic qubits and atomic memories [17, 18] due to their narrow bandwidths comparable to or even smaller than atomic natural linewidths [19–21]. In the typical double-Λ atomic system, biphotons can be efficiently generated via SFWM only if the pump field is far-detuned from a corresponding transition to well suppress the linear absorption and Raman gain [8–10]. Recently, we found however that the pump field could also work on resonance and hence be quite weak in generating biphotons [22] as a second pump field is introduced for creating a balanced dark state (DS) composed of two equally populated ground states [23].

Considering large nonlocal optical nonlinearities [5–7] that might be attained in Rydberg atoms, here we propose a scheme for the efficient generation of biphotons by exploiting an imbalanced DS that involves a weakly populated Rydberg state and a strongly populated ground state. This DS enables *both* a large suppression of the linear absorption and Raman gain by keeping the remaining three states empty, *and* a great enhancement of the SFWM process through nonlocal nonlinear susceptibilities that are two-order larger than their local counterparts due to *vdW* interactions. Both effects concur to a four-order enhancement of the generation rate of Stokes and anti-Stokes photon pairs, leading to the spectral brightness per pump power comparable to or larger than that observed in recent state-of-the-art experiments [24, 25] with higher optical depths.

Our set-up consists of a modified double-Λ atomic level configuration, see Fig. 1(a), with the *pump* field of frequency (amplitude) ω_p (E_p), the *coupling* field of frequency (amplitude) ω_c (E_c), and an additional *driving* field of frequency (amplitude) ω_d (E_d) applied on transitions $|1\rangle \leftrightarrow |4\rangle$, $|2\rangle \leftrightarrow |3\rangle$, and $|4\rangle \leftrightarrow |5\rangle$, respectively. The corresponding detunings (Rabi frequencies) are $\Delta_p = \omega_p - \omega_{41}$ ($\Omega_p = \mu_{41}E_p/2\hbar$), $\Delta_c = \omega_c - \omega_{32}$ ($\Omega_c = \mu_{32}E_c/2\hbar$), and $\Delta_d = \omega_d - \omega_{54}$ ($\Omega_d = \mu_{54}E_d/2\hbar$) with μ_{ij} being electric dipole moment on transition $|i\rangle \leftrightarrow |j\rangle$. A Stokes and an anti-Stokes field will be simultaneously generated with detunings (Rabi frequencies) $\Delta_s = \omega_s - \omega_{42}$ ($\Omega_s = \mu_{42}E_s/2\hbar$) and $\Delta_{as} = \omega_{as} - \omega_{31}$ ($\Omega_{as} = \mu_{31}E_{as}/2\hbar$) via SFWM [8]. Conservation of energy enforces $\delta_s = \Delta_p - \Delta_s$ and $\delta_{as} = \Delta_c - \Delta_{as}$ to cancel out, making it convenient to adopt two-photon detuning $\delta = \delta_s = -\delta_{as}$ as a frequency scale parameter.

Taking the upmost state $|5\rangle$ as a high Rydberg state, the total interaction Hamiltonian is ($\hbar = 1$)

$$\begin{aligned}\hat{H}_t = -\sum_{\alpha=1}^{N}[&(\Delta_p+\Delta_d)\hat{S}^{\alpha}_{55} + \Delta_p\hat{S}^{\alpha}_{44} + (\delta+\Delta_c)\hat{S}^{\alpha}_{33} \\ &+ \delta\hat{S}^{\alpha}_{22} + (\Omega_c\hat{S}^{\alpha}_{23} + \Omega_p\hat{S}^{\alpha}_{14} + \Omega_d\hat{S}^{\alpha}_{45} + \Omega_{as}\hat{S}^{\alpha}_{13} \\ &+ \Omega_s\hat{S}^{\alpha}_{24} + H.c.)] - \sum_{\beta<\alpha}^{N}\mathcal{V}(d_{\alpha\beta})\hat{S}^{\alpha}_{55}\otimes\hat{S}^{\beta}_{55},\end{aligned} \tag{1}$$

where $\hat{S}^{\alpha}_{ij} \equiv |j\rangle_{\alpha\alpha}\langle i|$ denotes the transition ($i \neq j$) or projection ($i = j$) operator of the αth atom; $\mathcal{V}(d_{\alpha\beta}) = C_6/d^6_{\alpha\beta}$ is the *vdW* potential responsible for the nonlocal interaction between the

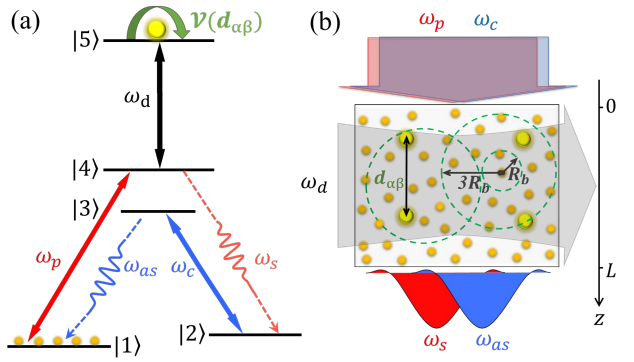

Fig. 1. Level configuration (a) and excitation geometry (b) proposed to observe enhanced biphoton generation in a Rydberg gas of ^{87}Rb atoms. Co-propagating pump (ω_p) and coupling (ω_c) fields generate Stokes (ω_s) and anti-Stokes (ω_{as}) photon pairs in the presence of two-body Rydberg interactions $\mathcal{V}(d_{\alpha\beta})$ that strongly enhance the nonlocal SFWM nonlinearities through a transverse driving (ω_d) field. The ^{87}Rb levels are selected as $|1\rangle = |5S_{1/2}, F = 1\rangle$, $|2\rangle = |5S_{1/2}, F = 2\rangle$, $|3\rangle = |5P_{1/2}, F = 1\rangle$, $|4\rangle = |5P_{1/2}, F = 2\rangle$, and $|5\rangle = |60S_{1/2}\rangle$. In our proposal, at most two atoms (*yellow filled circles*) can be excited to Rydberg state $|5\rangle$ in each sphere (*green dashed circles*) of radius $3R_b$ (see text) while most atoms (*orange filled circles*) remain in ground state $|1\rangle$. Decay rates are taken as $\Gamma_{32} = \Gamma_{31} = \Gamma_{42} = \Gamma_{41} = \gamma$ and $\Gamma_{54} = \Gamma_{53} = \gamma'$ while the dephasing rates are $\gamma_{ij} = \sum_k (\Gamma_{ik} + \Gamma_{jk})/2$.

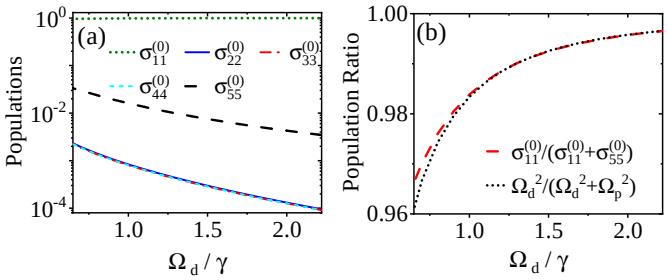

Fig. 2. Atomic populations (a) and dark-state population ratio (b) versus driving Rabi frequency Ω_d with $\Delta_c = \Delta_p = \Delta_d = 0$, $\Omega_c = 5\gamma$, $\Omega_p = 0.13\gamma$, and $\gamma = 2.873$ MHz. Other parameters are $\gamma' = 2.0$ kHz, $\mu_{eg} = 2.537 \times 10^{-29}$ Cm, $C_6 = 140$ GHz μm^6, $N_a = 1.0 \times 10^{10}$ cm^{-3}, and $L = 1.0$ mm.

αth and βth atoms at distance $d_{\alpha\beta}$ and in state $|5\rangle$.

An accurate description of the linear and nonlinear optical responses in the presence of Rydberg excitations requires a many-body approach [5–7]. To this purpose, we choose to first take the continuous operator $\hat{S}_{ij}(\mathbf{r})$ as an average of the discrete operator $\hat{S}_{ij}^{(\alpha)}$ over a small volume $\delta V(\mathbf{r})$ centered at position $\mathbf{r}$ and then use its expectation value to calculate the (local) one-body density matrix element $\sigma_{ij}(\mathbf{r}) = \langle \hat{S}_{ij}(\mathbf{r}) \rangle$. The same procedure applies to the (nonlocal) two-body density matrix element $\sigma_{ij,kl}(\mathbf{r}, \mathbf{r}') = \langle \hat{S}_{ij}(\mathbf{r}) \hat{S}_{kl}(\mathbf{r}') \rangle$, three-body density matrix element $\sigma_{ij,kl,mn}(\mathbf{r}, \mathbf{r}', \mathbf{r}'') = \langle \hat{S}_{ij}(\mathbf{r}) \hat{S}_{kl}(\mathbf{r}') \hat{S}_{mn}(\mathbf{r}'') \rangle$, etc. With the help of the evolution (Heisenberg) equation $i\partial_t \hat{S}_{ij} = [\hat{H}_t, \hat{S}_{ij}] + \mathcal{L}\hat{S}_{ij}$, where $\mathcal{L}$ is the Lindblad superoperator describing relevant dissipation processes, we find that the dynamics of $\sigma_{ij}(\mathbf{r})$ depends on $\sigma_{ij,kl}(\mathbf{r}, \mathbf{r}')$ via $\mathcal{V}_{ij,kl}^{\text{int}} = N_a \int d^3\mathbf{r}' \mathcal{V}(|\mathbf{r}' - \mathbf{r}|) \sigma_{ij,kl}(\mathbf{r}, \mathbf{r}')$. Likewise, the dynamics of $\sigma_{ij,kl}(\mathbf{r}, \mathbf{r}')$ depends on $\sigma_{ij,kl,mn}(\mathbf{r}, \mathbf{r}', \mathbf{r}'')$ via $\mathcal{V}_{ij,kl,mn}^{\text{int}} = N_a \int d^3\mathbf{r}'' \mathcal{V}(|\mathbf{r}'' - \mathbf{r}|) \sigma_{ij,kl,mn}(\mathbf{r}, \mathbf{r}', \mathbf{r}'')$, and so on. Here $d_{\alpha\beta}$ has been replaced by $|\mathbf{r}' - \mathbf{r}|$ or $|\mathbf{r}'' - \mathbf{r}|$ while N_a denotes the overall atomic density. Following this procedure, we arrive at a hierarchy of coupled equations that can, however, be truncated to keep only one-body and two-body density matrix elements. Although a similar framework of the many-body approach we follow here can be found elsewhere [7], the conditions under which a truncation occurs are now briefly discussed.

It is well known that at most one atom can be excited to the Rydberg state $|5\rangle$ within a sphere (blockade volume), as shown in Fig. 1(b), whose radius is determined by $R_b = [C_6(\Delta_d^2 + \gamma_{41}^2)^{1/2}/\Omega_d^2]^{1/6}$ in the limit of $\Omega_d \gg \Omega_p$ and $\Delta_d + \Delta_p = 0$ [3]. Hence, it is not necessary to calculate $\mathcal{V}_{ij,kl}^{\text{int}}$ and other *vdW* integrals inside each blockade volume with a very small Rydberg population, *i.e.* $\frac{4}{3}\pi N_a R_b^3 \sigma_{55} \ll 1$, nevertheless an integration outside the blockade volume is appropriate and ranging from $|\mathbf{r}' - \mathbf{r}| = R_b$ up to $|\mathbf{r}' - \mathbf{r}| = 3R_b$ because $\mathcal{V}(3R_b) = \mathcal{V}(R_b)/729$ is already negligible. In this case, the truncation at two-body *vdW* interactions mentioned above is valid provided $\frac{4}{3}\pi N_a (3R_b)^3 \sigma_{55} < 2$ [7] for a moderate density N_a.

Steady-state solutions of the one-body and two-body dynamic equations can be easily attained by setting $\partial_t \sigma_{ij}(\mathbf{r}) = \partial_t \sigma_{ij,kl}(\mathbf{r}, \mathbf{r}') = 0$. As we are just interested in the SFWM processes generating very weak Stokes and anti-Stokes fields, it is appropriate to adopt the standard perturbation method [5–7] that entails the expansion of $\sigma_{ij}(\mathbf{r}) = \sum_{n=0}^{\infty} \sigma_{ij}^{(n)}(\mathbf{r})$ and $\sigma_{ij,kl}(\mathbf{r}, \mathbf{r}') = \sum_{n=0}^{\infty} \sigma_{ij,kl}^{(n)}(\mathbf{r}, \mathbf{r}')$ with respect to Ω_s and Ω_{as}. For our purpose, one-body equations require zero-order and first-order solutions but two-body equations require only zero-order solutions. These solutions clearly depend on the decay rates γ and γ' as well as dephasings γ_{ij} (see Fig. 1(a)).

Zero-order solutions are attained when neither Stokes nor anti-Stokes photons are present, whereby our five-level system can be regarded as an incoherent combination of the subsystem of three levels $\{|1\rangle, |4\rangle, |5\rangle\}$ and the subsystem of two levels $\{|2\rangle, |3\rangle\}$. In the absence of *vdW* interactions, the former subsystem will exhibit a dark state $|D\rangle = (\Omega_d|1\rangle - \Omega_p|5\rangle)/(\Omega_d^2 + \Omega_p^2)^{1/2}$ [23] under two-photon resonance $\Delta_d + \Delta_p = 0$. In the presence of *vdW* interactions, however, populations and coherence in the ground and Rydberg states must deviate from those predicted by the dark state and take the form

$$\begin{aligned} \sigma_{11}^{(0)} &\simeq \frac{\Omega_d^2}{\Omega_p^2 + \Omega_d^2} + f(\mathcal{V}_{55,51}^{\text{int}}, \mathcal{V}_{55,15}^{\text{int}}), \\ \sigma_{55}^{(0)} &\simeq \frac{\Omega_p^2}{\Omega_p^2 + \Omega_d^2} + g(\mathcal{V}_{55,51}^{\text{int}}, \mathcal{V}_{55,15}^{\text{int}}), \\ \sigma_{51}^{(0)} &\simeq \frac{-\Omega_d \Omega_p}{\Omega_p^2 + \Omega_d^2} + h(\mathcal{V}_{55,51}^{\text{int}}, \mathcal{V}_{55,15}^{\text{int}}), \end{aligned} \tag{2}$$

where f, g, and h denote (small) perturbations due to $|\mathcal{V}_{55,51}^{\text{int}} = \mathcal{V}_{55,15}^{\text{int}*}| \simeq 0.01\gamma \ll \Omega_{p,d}$ for the parameters used in our following calculations, while the contributions arising from $\mathcal{V}_{55,54}^{\text{int}} = \mathcal{V}_{55,45}^{\text{int}*}$ have been neglected based on the fact that $|\sigma_{55,51}^{(0)}(\mathbf{r}, \mathbf{r}')| \gg |\sigma_{55,14}^{(0)}(\mathbf{r}, \mathbf{r}')| \gg |\sigma_{55,54}^{(0)}(\mathbf{r}, \mathbf{r}')|$ and $\sigma_{11}^{(0)} \gg \sigma_{55}^{(0)} \gg \sigma_{44}^{(0)}$.

Numerical calculations reported in Fig. 2(a) show that populations are primarily distributed in the ground $|1\rangle$ and Rydberg

$|5\rangle$ states, with the other three states almost empty. Small deviations of the actual atomic state from an ideal dark state, with $\sigma_{11}^{(0)}/(\sigma_{11}^{(0)}+\sigma_{55}^{(0)})$ slightly different from $\Omega_d^2/(\Omega_d^2+\Omega_p^2)$ and with departures being more pronounced at smaller Ω_d's, are instead shown in Fig. 2(b). These results confirm that the dark state is modified just a little by the *vdW* interactions.

First-order solutions $\sigma_{31}^{(1)}$ and $\sigma_{42}^{(1)}$ answer for the linear absorption (gain) and dispersion as well as the nonlinear SFWM generation of both Stokes and anti-Stokes fields, respectively. They can be attained by taking zero-order solutions $\sigma_{ij}^{(0)}$ into steady-state equations of first-order elements $\sigma_{ij}^{(1)}$. With $\sigma_{31}^{(1)}$ and $\sigma_{42}^{(1)}$, we have the Stokes and anti-Stokes polarizations

$$\begin{aligned} P_{31} &= N_a\mu_{13}\sigma_{31}^{(1)} = \epsilon_0\chi_{as}^{(1)}E_{as} + \epsilon_0\chi_{as,s}^{(3)}E_pE_cE_s^*, \\ P_{42} &= N_a\mu_{24}\sigma_{42}^{(1)} = \epsilon_0\chi_{s}^{(1)}E_{s} + \epsilon_0\chi_{s,as}^{(3)}E_pE_cE_{as}^*, \end{aligned} \tag{3}$$

where $\chi_{as}^{(1)}$ and $\chi_{s}^{(1)}$ denote the linear susceptibilities while $\chi_{as,s}^{(3)}$ and $\chi_{s,as}^{(3)}$ denote the nonlinear susceptibilities. They are functions of $\mathcal{V}_{55,51}^{\rm int}=\mathcal{V}_{55,15}^{\rm int*}$ through zero-order solutions $\sigma_{ij}^{(0)}$, hence can be divided into a *local* component determined solely by atom-field interactions and a *nonlocal* component depending also on *vdW* interactions, i.e. $\chi_{as}^{(1)}=\chi_{as}^{(1l)}+\chi_{as}^{(1n)}$, $\chi_{s}^{(1)}=\chi_{s}^{(1l)}+\chi_{s}^{(1n)}$, $\chi_{as,s}^{(3)}=\chi_{as,s}^{(3l)}+\chi_{as,s}^{(3n)}$, and $\chi_{s,as}^{(3)}=\chi_{s,as}^{(3l)}+\chi_{s,as}^{(3n)}$ with l and n indicating 'local' and 'nonlocal', respectively. Numerical calculations (not reported here) confirm that loss for the anti-Stokes photons due to linear absorption with $\mathtt{Im}(\chi_{as}^{(1)})>0$ and noise for the Stokes photons due to Raman scattering with $\mathtt{Im}(\chi_{s}^{(1)})<0$ are negligible even in the presence of *vdW* interactions because, for the used parameters, $\chi_{as}^{(1)}$ and $\chi_{s}^{(1)}$ are at least one-order of magnitude smaller than $\chi_{as,s}^{(3)}E_pE_c$ and $\chi_{s,as}^{(3)}E_pE_c$.

Then we turn to the nonlinear susceptibilities $\chi_{as,s}^{(3)}$ and $\chi_{s,as}^{(3)}$ accounting for the correlated generation of Stokes and anti-Stokes photon pairs, each of which can be divided into a local and a nonlocal component once again. In the case of $\{\gamma',\Omega_p\}\ll\{\gamma,\Omega_{c,d}\}$, if all light fields work near or on resonance, the local components become

$$\begin{aligned} \chi_{as,s}^{(3l)} &\simeq K\frac{-i\gamma_{51}/\Omega_d^2}{(\delta+i\gamma_{e1}+\Omega_{e1})(\delta+i\gamma_{e1}-\Omega_{e1})}, \\ \chi_{s,as}^{(3l)} &\simeq K\frac{-i\gamma_{51}/\Omega_d^2}{(\delta-i\gamma_{e2}+\Omega_{e2})(\delta-i\gamma_{e2}-\Omega_{e2})}, \end{aligned} \tag{4}$$

while the nonlocal components are

$$\begin{aligned} \chi_{as,s}^{(3n)} &\simeq K\frac{-\mathcal{V}_{55,51}^{\rm int}/\Omega_d\Omega_p}{(\delta+i\gamma_{e1}+\Omega_{e1})(\delta+i\gamma_{e1}-\Omega_{e1})}, \\ \chi_{s,as}^{(3n)} &\simeq K\frac{-\mathcal{V}_{55,51}^{\rm int}/\Omega_d\Omega_p}{(\delta-i\gamma_{e2}+\Omega_{e2})(\delta-i\gamma_{e2}-\Omega_{e2})}, \end{aligned} \tag{5}$$

with $\Omega_{e1}=[\Omega_c^2-(\gamma_{21}-\gamma_{31})^2/4]^{1/2}$, $\gamma_{e1}=(\gamma_{21}+\gamma_{31})/2$, $\Omega_{e2}=[\Omega_c^2-(\gamma_{42}-\gamma_{43})^2/4]^{1/2}$, $\gamma_{e2}=(\gamma_{42}+\gamma_{43})/2$, and $K=N_a\mu_{14}\mu_{24}\mu_{23}\mu_{13}/4\hbar^3\epsilon_0$. A direct comparison of Eqs. (4) and (5) shows that $|\chi_{as,s}^{(3n)}/\chi_{as,s}^{(3l)}|$ and $|\chi_{s,as}^{(3n)}/\chi_{s,as}^{(3l)}|$ scale as $(\Omega_d/\Omega_p)\times(|\mathcal{V}_{55,51}^{\rm int}|/\gamma_{51})$, which is on the order of 10^2 for the typical parameters used here. Numerical calculations (not reported here) confirm that $\chi_{as,s}^{(3)}$ and $\chi_{s,as}^{(3)}$ exhibit a two-order of magnitude enhancement with respect to the corresponding local ones.

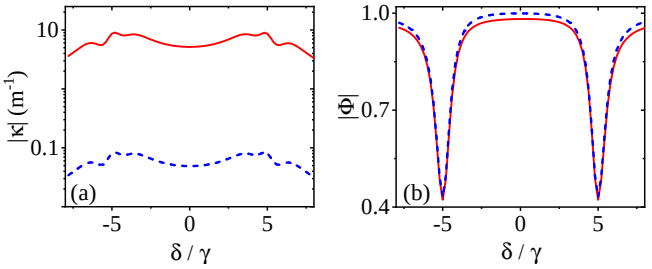

Fig. 3. Absolute values of wave-mixing function (a) and phase-mismatch factor (b). Blue-dashed lines are attained with only local susceptibilities. Parameters are the same as in Fig. 2 except $\lambda_p\simeq\lambda_c\simeq\lambda_s\simeq\lambda_{as}\simeq 795.0$ nm and $\Omega_d=1.3\gamma$.

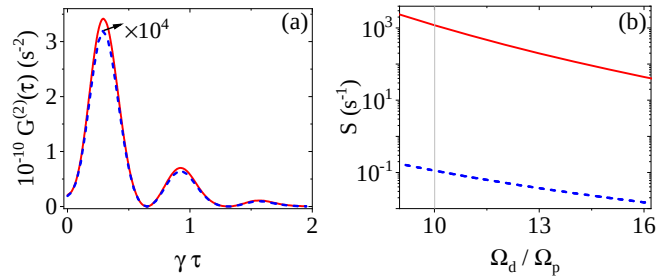

Fig. 4. Intensity correlation function (a) and biphoton generation rate (b). Blue-dashed lines are attained with only local susceptibilities while vertical gray line in (b) refers to the point where (a) is calculated. Parameters are the same as in Fig. 3.

We consider now the situation where the pump and coupling fields co-propagate along the **z** direction and are transverse to the driving field (see Fig. 1(b)). To examine the biphoton generation, we express $E_s^*\to\hat{E}_s^\dagger\to\hat{a}_s^\dagger$ and $E_{as}^*\to\hat{E}_{as}^\dagger\to\hat{a}_{as}^\dagger$ [10] in terms of annihilation operators $\hat{a}_s$ and $\hat{a}_{as}$, respectively, for the Stokes and anti-Stokes fields. The effective Hamiltonian that describes the generation of Stokes and anti-Stokes photons co-propagating (*phase matching*) along the **z** direction reads

$$\hat{H}_I=\frac{\epsilon_0 A}{4}\int_0^L dz[(\chi_{as,s}^{(3)}+\chi_{s,as}^{(3)})E_cE_p\hat{E}_s^\dagger\hat{E}_{as}^\dagger]+H.c., \tag{6}$$

where A and L are the atomic sample's cross-section area and length. SFWM nonlinear generation [10] (to the first-order) results into the following biphoton state,

$$|\Psi\rangle=L\int d\delta\kappa(\delta)\Phi(\delta)\hat{a}_s^\dagger(\delta)\hat{a}_{as}^\dagger(\delta)|0_s,0_{as}\rangle, \tag{7}$$

where $\kappa=-i\sqrt{\omega_{as}\omega_s}(\chi_{as,s}^{(3)}+\chi_{s,as}^{(3)})E_pE_c/2c$ is the wave-mixing function and $\Phi=\exp(-i\Delta kL/2)\mathrm{sinc}(\Delta kL/2)$ the complex phase-mismatch factor. Note that $\omega_s=\omega_p-\omega_{21}$ ($\omega_{as}=\omega_c+\omega_{21}$) denotes the central frequency of a Stokes (anti-Stokes) photon, while $\Delta k=k_s^*+k_{as}^*-k_p-k_c$ refers to the wavevector mismatch with $k_j=\sqrt{1+\chi_j}2\pi/\lambda_j$. As depicted in Fig. 3(a), $|\kappa|$ is significantly enhanced by two-body Rydberg correlations in that $|\chi_{as,s}^{(3n)}|$ and $|\chi_{s,as}^{(3n)}|$ are two-order larger than $|\chi_{as,s}^{(3l)}|$ and $|\chi_{s,as}^{(3l)}|$. We observe from Fig. 3(b), however, that $|\Phi|$ depends weakly on two-body Rydberg correlations in that $|\chi_{as}^{(1)}|$ and $|\chi_{s}^{(1)}|$ remain small even with *vdW* interactions.

Next, we examine the intensity correlation function of a Stokes and an anti-Stokes photon generated at times t_s and t_{as}, respectively. This function is proportional to the squared modulus of a Fourier transform on the product $\kappa \times \Phi$ with respect to $\tau = t_{as} - t_s$ as given below

$$G^{(2)}(\tau) = \frac{L^2}{4\pi^2} \left| \int d\delta \kappa(\delta) \Phi(\delta) e^{i(k_s + k_{as})L} e^{-i\delta\tau} \right|^2, \qquad (8)$$

from which we can calculate the biphoton generation rate $S = \int d\tau G^{(2)}(\tau)$. Similarly, we can compute the individual (photon) generation rates $R_j = \frac{L^2}{2\pi} \int d\delta f_j(\delta) \left|\kappa(\delta)\Phi(\delta)\right|^2$ [9] with $f_j(\delta) = e^{-\mathrm{Im}\chi_j(\delta)\omega_j L/c}$ for $j \in \{s, as\}$. Fig. 4 shows that values of $G^{(2)}(\tau)$ over 10^{10} s^{-2} and S up to 10^3 s^{-1} are possible, with the contributions (red-solid) from nonlocal vdW interactions being nearly four-order of magnitude larger than those (blue-dashed) from local ones. The decrease of S with the increase of Ω_d, restricted here by $\Omega_d/\Omega_p > 9$ to ensure both $\sigma_{55}^{(0)}/\sigma_{11}^{(0)} \lesssim 0.01$ and $\sigma_{11}^{(0)} \simeq 1.0$ [cf. Eq. (2)], is primarily due to $\chi_{s,as}^{(3n)} \propto -\mathcal{V}_{55,51}^{\mathtt{int}}/\Omega_d$ and $\chi_{as,s}^{(3n)} \propto -\mathcal{V}_{55,51}^{\mathtt{int}}/\Omega_d$ together with the implicit dependence of $\mathcal{V}_{55,51}^{\mathtt{int}}$ on Ω_d through $\sigma_{55,51}^{(0)}$. The normalized cross-correlation function $g_{s,as}^{(2)}(\tau) = G^{(2)}(\tau)/R_s R_{as}$, needed to quantify the nonclassical properties, can be computed and it is found to violate the Cauchy-Schwarz inequality in excess of 10^4. These results are attained with an optical depth $\mathtt{OD} = 2\pi L\alpha/\lambda_{as} = 2\pi L\beta/\lambda_s \simeq 3.0$ ($\alpha = N_a\mu_{13}^2/\hbar\epsilon_0\gamma_{31}$ and $\beta = N_a\mu_{24}^2/\hbar\epsilon_0\gamma_{42}$), much lower than those used in previous schemes not involving Rydberg interactions [26–28].

A practical and important figure of merit is the generated spectral brightness per pump power or $\mathtt{GSBP} = S/P_p W_b$, which we compute here for $\Omega_p = 0.13\gamma$, $\Omega_c = 5\gamma$, and $\Omega_d = 1.3\gamma$ as well as a fixed optical depth $\mathtt{OD} \simeq 3.0$. If $P_p = 2\pi r_p^2 \hbar^2 \Omega_p^2 \epsilon_0 c/\mu_{51}^2$ denotes the pump power, with r_p being radius of the pump beam and $W_b \simeq 2\gamma$ being the spectral width, i.e. the full width at half maximum of a Fourier transform of $G^{(2)}(\tau)$, we estimate $\mathtt{GSBP} \simeq 4.5 \times 10^{10}$ pairs/(s mW MHz) at a power $P_p = 4.6$ pW for a very small beam radius ($r_p \simeq 1.7$ μm) and $\mathtt{GSBP} \simeq 1.3 \times 10^5$ pairs/(s mW MHz) at a power $P_p = 1.6$ μW for a larger radius ($r_p \simeq 1.0$ mm). The former ought to be compared to values of $\mathtt{GSBP} \simeq 2.0 \times 10^9$ pairs/(s mW MHz) as obtained e.g. in [24] for the same pump geometry ($r_p \simeq 1.7$ μm) though at densities $\mathtt{OD} = 40 \sim 80$ while the latter compared to values of $\mathtt{GSBP} \simeq 1.2 \times 10^6$ pairs/(s mW MHz) as obtained e.g. in [25] for the same geometry ($r_p \simeq 1.0$ mm) and at an even larger density $\mathtt{OD} = 110$. Note that we may access larger optical densities also within our scheme by directly increasing L (N_a fixed), which would lead to bigger $\mathtt{GSBP}$ values. At densities e.g. $\mathtt{OD} \simeq 15$ and the same pump powers as in the two cases above, one would anticipate $\mathtt{GSBP} \simeq 5.9 \times 10^{11}$ pairs/(s mW MHz) and $\mathtt{GSBP} \simeq 1.7 \times 10^6$ pairs/(s mW MHz), both corresponding to $S \simeq 1.6 \times 10^4$ s^{-1} and outdoing the brightnesses in [24, 25].

The relative ease with which one could control our set-up [12–16] would also allow for the development of a practical source of entanglement. Through a suitable gating of the photon pairs, *viz.* emission to a specific symmetry choice of the ground hyperfine states, and the use of a counter-propagating pump and coupling geometry we expect our scheme to be suitable to high-rate generation of polarization entanglement with photons (naturally) exhibiting linewidths and wavelengths compatible with atomic memory and photonic interconnects.

Our proposal for generating biphotons via SFWM in cold atoms hinges on vdW-type Rydberg interactions and benefits from an imbalanced dark state. The nonlocal vdW interactions lead to a significant enhancement of nonlinear susceptibilities hence a four-order of magnitude increase in the generation rate of nonclassically correlated Stokes and anti-Stokes photons. Very high generated spectral brightness per pump power, in turn, are anticipated as all light fields work on resonance.

Funding. National Key Research and Development Program of China (2021YFE0193500), National Natural Science Foundation of China (12074061), and Italian PNRR MUR (PE0000023-NQSTI).

Disclosures. The authors declare no conflicts of interest.

Data Availability Statement. Data underlying the results are available from the authors upon reasonable request.

REFERENCES

1. M. Saffman, T. G. Walker, and K. Mølmer, Rev. Mod. Phys. **82**, 2313 (2010).
2. C. S. Admas, J. D. Pritchard, and J. P. Shaffer, J. Phys. B: At. Mol. Opt. Phys. **53**, 012002 (2020).
3. D. Petrosyan, J. Otterbach, and M. Fleischhauer, Phys. Rev. Lett. **107**, 213601 (2011).
4. T. E. Lee, H. Häffner, and M. C. Cross, Phys. Rev. A **84**, 031402(R) (2011).
5. Z. Y. Bai and G. X. Huang, Opt. Express **24**, 4442 (2016).
6. Z. Y. Bai, W. B. Li, and G. X. Huang, Optica **6**, 309 (2019).
7. D.-D. Zheng, H.-M. Zhao, X.-J. Zhang, and J.-H. Wu, Phys. Rev. A **106**, 043119 (2022).
8. V. Balić, D. A. Braje, P. Kolchin, G. Y. Yin, and S. E. Harris, Phys. Rev. Lett. **94**, 183601 (2005).
9. P. Kolchin, Phys. Rev. A **75**, 033814 (2007).
10. S. Du, J. Wen, and M. H. Rubin, J. Opt. Soc. Am. B **25**, C98 (2008).
11. A. Zavatta, M. Artoni, and G. La Rocca, Phys. Rev. A **99**, 031802(R) (2019).
12. L. Zhao, X. Guo, C. Liu, Y. Sun, M. M. T. Loy, and S. Du, Optica **1**, 84 (2014).
13. X. J. Zhang, J. H. Wu, G. C. La Rocca, and M. Artoni, Opt. Express **28**, 31076 (2020).
14. T. Jeong and H. S. Moon, Opt. Express **28**, 3985 (2020).
15. C. Wang, C.-H. Lee, and Y.-H. Kim, Opt. Express **27**, 34611 (2019).
16. K. Liao, H. Yan, J. He, S. Du, Z.-M. Zhang, and S.-L. Zhu, Phys. Rev. Lett. **112**, 243602 (2014).
17. L. M. Duan, M. D. Lukin, J. I. Cirac, and P. Zoller, Nature **414**, 413 (2001).
18. C. H. van der Wal, M. D. Eisaman, A. André, R. L. Walsworth, D. F. Phillips, A. S. Zibrov, and M. D. Lukin, Science **301**, 196 (2003).
19. B. Srivathsan, G. K. Gulati, B. Chng, G. Maslennikov, D. Matsukevich, and C. Kurtsiefer, Phys. Rev. Lett. **111**, 123602 (2013).
20. H. Yan, S. Zhang, J. F. Chen, M. M. T. Loy, G. K. L. Wong, and S. Du, Phys. Rev. Lett. **106**, 033601 (2011).
21. T.-M. Zhao, Y. S. Ihn, and Y.-H. Kim, Phys. Rev. Lett. **122**, 123607 (2019).
22. H.-M. Zhao, X.-J. Zhang, M. Artoni, G. La Rocca, and J.-H. Wu, Phys. Rev. A **106**, 023711 (2022).
23. M. Fleischhauer, A. Imamoglu, and J. P. Marangos, Rev. Mod. Phys. **77**, 633 (2005).
24. A. Bruns, C.-Y. Hsu, S. Stryzhenko, E. Giese, L. P. Yatsenko, I. A. Yu, T. Halfmann and T. Peters, Quantum Sci. Technol. **8**, 015002 (2023).
25. Y.-S. Wang, K.-B. Li, C.-F. Chang, T.-W. Lin, J.-Q. Li, S.-S. Hsiao, J.-M. Chen, Y.-H. Lai, Y.-C. Chen, Y.-F. Chen, C.-S. Chuu, and I. A. Yu, APL Photonics **7**, 126102 (2022).
26. S. Du, P. Kolchin, C. Belthangady, G.Y. Yin, and S.E. Harris, Phys. Rev. Lett. **100**, 183603 (2008).
27. L. Zhao, X. Guo, Y. Sun, Y. Su, M.M.T. Loy, and S. Du, Phys. Rev. Lett. **115**, 193601 (2015).
28. L. Zhao, Y. Su, and S. Du, Phys. Rev. A **93**, 033815 (2016).

REFERENCES

1. M. Saffman, T. G. Walker, and K. Mølmer, Quantum information with Rydberg atoms, Rev. Mod. Phys. **82**, 2313 (2010).
2. C. S. Admas, J. D. Pritchard, and J. P. Shaffer, Rydberg atom quantum technologies, J. Phys. B: At. Mol. Opt. Phys. **53**, 012002 (2020).
3. D. Petrosyan, J. Otterbach, and M. Fleischhauer, Electromagnetically induced transparency with Rydberg atoms, Phys. Rev. Lett. **107**, 213601 (2011).
4. T. E. Lee, H. Häffner, and M. C. Cross, Antiferromagnetic phase transition in a nonequilibrium lattice of Rydberg atoms, Phys. Rev. A **84**, 031402(R) (2011).
5. Z. Y. Bai and G. X. Huang, Enhanced third-order and fifth-order Kerr nonlinearities in a cold atomic system via Rydberg-Rydberg interaction, Opt. Express **24**, 4442 (2016).
6. Z. Y. Bai, W. B. Li, and G. X. Huang, Stable single light bullets and vortices and their active control in cold Rydberg gases, Optica **6**, 309-317 (2019).
7. D.-D. Zheng, H.-M. Zhao, X.-J. Zhang, and J.-H. Wu, Correlation-enhanced Goos-Hänchen shift in Rydberg atomic gases, Phys. Rev. A **106**, 043119 (2022).
8. V. Balić, D. A. Braje, P. Kolchin, G. Y. Yin, and S. E. Harris, Generation of paired photons with controllable waveforms, Phys. Rev. Lett. **94**, 183601 (2005).
9. P. Kolchin, Electromagnetically-induced-transparency-based paired photon generation, Phys. Rev. A **75**, 033814 (2007).
10. S. Du, J. Wen, and M. H. Rubin, Narrowband biphoton generation near atomic resonance, J. Opt. Soc. Am. B **25**, C98 (2008).
11. A. Zavatta, M. Artoni, and G. La Rocca, Engineering of heralded narrowband color-entangled states, Phys. Rev. A **99**, 031802(R) (2019).
12. L. Zhao, X. Guo, C. Liu, Y. Sun, M. M. T. Loy, and S. Du, Photon pairs with coherence time exceeding 1 μs, Optica **1**, 84 (2014).
13. X. J. Zhang, J. H. Wu, G. C. La Rocca, and M. Artoni, Efficient generation of heralded narrowband color-entangled states, Opt. Express **28**, 31076-31092 (2020).
14. T. Jeong and H. S. Moon, Temporal- and spectral-property measurements of narrowband photon pairs from warm double-Λ type atomic ensemble, Opt. Express **28**, 3985 (2020).
15. C. Wang, C.-H. Lee, and Y.-H. Kim, Generation and characterization of position-momentum entangled photon pairs in a hot atomic gas cell, Opt. Express **27**, 34611 (2019).
16. K. Liao, H. Yan, J. He, S. Du, Z.-M. Zhang, and S.-L. Zhu, Subnatural-linewidth polarization-entangled photon pairs with controllable temporal length, Phys. Rev. Lett. **112**, 243602 (2014).
17. L. M. Duan, M. D. Lukin, J. I. Cirac, and P. Zoller, Long-distance quantum communication with atomic ensembles and linear optics, Nature **414**, 413 (2001).
18. C. H. van der Wal, M. D. Eisaman, A. André, R. L. Walsworth, D. F. Phillips, A. S. Zibrov, and M. D. Lukin, Atomic memory for correlated photon states, Science **301**, 196 (2003).
19. B. Srivathsan, G. K. Gulati, B. Chng, G. Maslennikov, D. Matsukevich, and C. Kurtsiefer, Narrow band source of transform-limited photon pairs via four-wave mixing in a cold atomic ensemble, Phys. Rev. Lett. **111**, 123602 (2013).
20. H. Yan, S. Zhang, J. F. Chen, M. M. T. Loy, G. K. L. Wong, and S. Du, Generation of narrow-band hyperentangled nondegenerate paired photons, Phys. Rev. Lett. **106**, 033601 (2011).
21. T.-M. Zhao, Y. S. Ihn, and Y.-H. Kim, Direct generation of narrow-band hyperentangled photons, Phys. Rev. Lett. **122**, 123607 (2019).
22. H.-M. Zhao, X.-J. Zhang, M. Artoni, G. La Rocca, and J.-H. Wu, Photon-pair generation on resonance via a dark state, Phys. Rev. A **106**, 023711 (2022).
23. M. Fleischhauer, A. Imamoglu, and J. P. Marangos, Electromagnetically induced transparency: Optics in coherent media, Rev. Mod. Phys. **77**, 633 (2005).
24. A. Bruns, C.-Y. Hsu, S. Stryzhenko, E. Giese, L. P. Yatsenko, I. A. Yu, T. Halfmann and T. Peters, Ultrabright and narrowband intra-fiber biphoton source at ultralow pump power, Quantum Sci. Technol. **8**, 015002 (2023).
25. Y.-S. Wang, K.-B. Li, C.-F. Chang, T.-W. Lin, J.-Q. Li, S.-S. Hsiao, J.-M. Chen, Y.-H. Lai, Y.-C. Chen, Y.-F. Chen, C.-S. Chuu, and I. A. Yu, Temporally ultralong biphotons with a linewidth of 50 kHz, APL Photonics **7**, 126102 (2022).
26. S. Du, P. Kolchin, C. Belthangady, G.Y. Yin, and S.E. Harris, Subnatural linewidth biphotons with controllable temporal length, Phys. Rev. Lett. **100**, 183603 (2008).
27. L. Zhao, X. Guo, Y. Sun, Y. Su, M.M.T. Loy, and S. Du, Shaping the biphoton temporal waveform with spatial light modulation, Phys. Rev. Lett. **115**, 193601 (2015).
28. L. Zhao, Y. Su, and S. Du, Narrowband biphoton generation in the group delay regime, Phys. Rev. A **93**, 033815 (2016).